Impact of mass uncertainties of ^{83,84}Mo, ^{82}Nb and ^{80}Zr on the rp-process nucleosynthesis*

Jia-Hao Lv (吕佳浩)[1,2] Yuan-Ming Xing (邢元明)[1†] Meng Wang (王猛)[1] Yu-Hu Zhang (张玉虎)[1]

[1]CAS Key Laboratory of High-Precision Nuclear Spectroscopy, Institute of Modern Physics, Chinese Academy of Sciences, Lanzhou 730000, China
[2]School of Nuclear Science and Technology, University of Chinese Academy of Sciences, Beijing 100049, China

Abstract: Precise nuclear mass values are key parameters for modeling astrophysical X-ray bursts. In this work, we investigate the impact of current mass uncertainties of ^{83,84}Mo, ^{82}Nb, and ^{80}Zr on the nucleosynthesis of the rp-process. The results reveal that the impact of the mass uncertainties of ^{83,84}Mo and ^{80}Zr on the final abundances is negligible, although the large mass uncertainty of ^{83}Mo can reach a level close to 1 MeV. In contrast, the final abundances are highly sensitive to the mass value of ^{82}Nb. An increase in the mass of ^{82}Nb can significantly enhance the abundance at $A = 81$. Furthermore, the Zr-Nb cycle in the rp-process is investigated and confirmed to play a minor role in the rp-process flows.

Keywords: abundances, nucleosynthesis, X-ray burst (XRB), mass excess

DOI: 10.1088/1674-1137/ae71a7 **CSTR:** 32044.14.ChinesePhysicsC.50084114

I. INTRODUCTION

Type I X-ray bursts (XRBs) are thermonuclear phenomena characterized by a rapid increase in X-ray luminosity over a short duration (10−100 s). These bursts occur on the surfaces of neutron stars in low-mass X-ray binaries and provide deep insights into the properties of neutron stars [1]. As a neutron star accretes hydrogen- and helium-rich material from its companion star, an extreme environment of high temperature (T~10^8−10^9 K) and density (ρ~10^6 g/cm^3) is created. This extreme environment triggers a thermonuclear explosion in the accreted material, leading to thermal X-ray emission from the dramatically heated neutron star photosphere [2]. The nuclear reaction sequences powering these bursts include the 3α-reaction, the αp-process, and the rapid proton-capture process (rp-process). Among these, the rp-process is a key pathway for heavy-element nucleosynthesis [3−7].

Nuclear masses can significantly affect the light curves, reaction pathways, and final composition of nuclear ashes in the rp-process [8−10]. For nuclides with unknown masses, theoretical predictions or extrapolations are typically adopted, such as the finite-range droplet model (FRDM2012) [11], the Weizsäcker-Skyrme model (WS4) [12], the deformed relativistic Hartree–Bogoliubov theory in continuum (DRHBc) [13], and the Atomic Mass Evaluation (AME2020) [14]. However, differences in the mass values predicted by various mass models can reach the MeV level [15], whereas the mass uncertainties of key nuclides in the rp-process are generally required to be on the order of 50 keV [10] or even as low as 10 keV [8, 9]. For example, the first precise mass measurement and improved precision for a series of nuclides around ^{64}As [16] and ^{26}P [17] have provided deeper insights into the main reaction pathways and produced elements in the rp-process.

In the proton-rich region around mass number A~80, numerous nuclides had either unknown masses or large mass uncertainties [18, 19], despite playing a critical role in the rp-process [9]. Over the past few years, many experimental studies have provided new mass values in this region [20−23]. Nevertheless, there are still some nuclides, such as ^{83,84}Mo, ^{82}Nb, and ^{80}Zr, with only predicted masses or mass uncertainties much larger than 10 keV, as shown in Fig. 1. The corresponding effects on the nucleosynthesis of the rp-process have not yet been specifically investigated.

Furthermore, a proposed Zr-Nb cycle in this region, as illustrated in Fig. 1, can exert a considerable influence on rp-process nucleosynthesis [4, 24]. Although the Zr-Nb cycle has been claimed to be excluded on the basis of the experimentally determined S_α of 1.434(83) MeV for ^{84}Mo [23], the extent and conditions under which the Zr-Nb cycle can be excluded remain unclear—particularly given that a mass uncertainty of 80 keV still exists for

Received 4 March 2026; Accepted 19 May 2026; Accepted manuscript online 20 May 2026

* Supported by the National Key R&D Program of China (2023YFA1606401), the Youth Innovation Promotion Association of the Chinese Academy of Sciences (2021419), the NSFC (12135017, 12475128, 11961141004, 12121005) and the CAS Project for Young Scientists in Basic Research (YSBR-002)

† E-mail: xym@impcas.ac.cn

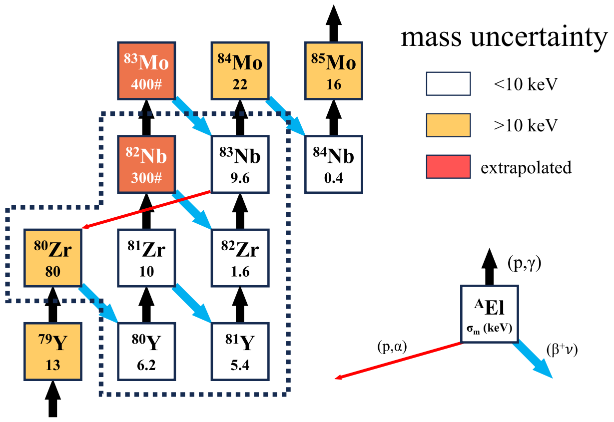

Fig. 1. (color online) Schematic rp-process path near A~80. The key relates an arrow to a specific interaction. The uncertainty of the mass excess is presented below the symbol of a nuclide. The values with symbol # are from the extrapolations in AME2020 [14]. The dotted line in the figure highlights the group of nuclides involved in the so-called Zr-Nb cycle [4].

^{80}Zr.

In this paper, we first study the impact of the current mass uncertainties of ^{83,84}Mo, ^{82}Nb, and ^{80}Zr on the composition of the nuclear ashes in XRBs. Then, we clarify the potential influence of the Zr-Nb cycle on the rp-process given the current mass values and uncertainties.

II. THE SENSITIVITY STUDY OF THE EFFECTS OF MASS UNCERTAINTIES

To explore the impact of nuclear masses on rp-process nucleosynthesis, reaction network calculations were carried out using the one-zone post-processing code NucNet [25]. The XRB model follows the approach of Schatz *et al.* [26], with initial mass fractions of accreted hydrogen and helium of $X^0_{\rm H} = 0.645$ and $X^0_{^4{\rm He}} = 0.355$, respectively. The ignition temperature was set to 0.23 GK at a density of 1.08×10^6 g/cm^3. The burst phase lasted 4 seconds, reaching a peak temperature of 1.9 GK, followed by a cooling phase that persisted for 200 seconds.

The nuclides studied in the network calculation are listed in Table 1. First, for each nuclide, the mass was independently varied by ± 2σ. The corresponding reaction rates were then calculated using the TALYS code [27], and the reverse reaction rates were determined by the NucNet code based on detailed balance principles and the reaction Q-values. Finally, the resulting abundances were compared with those obtained using the central mass value to assess the influence of each mass uncertainty on the ash composition.

Figure 2 shows, as a function of mass number A, the fractional difference, defined as the change in abundance relative to the results obtained using the AME2020 central mass values. It is evident that the ± 2σ mass variations of all studied nuclides, except ^{82}Nb, have a negligible impact on the abundances.

Table 1. The nuclear masses of interest studied in the network calculations. Also listed are the corresponding proton separation energies (S_p). The symbol # denotes extrapolated value from AME2020.

Nuclide	Mass excess/keV	S_p/keV
^{84}Mo	−54137(22) [23]	3797(25)
^{83}Mo	−46340(400)# [14]	1820(500)#
^{82}Nb	−51810(300)# [14]	1540(301)#
^{80}Zr	−55128(80) [22]	4433(82)

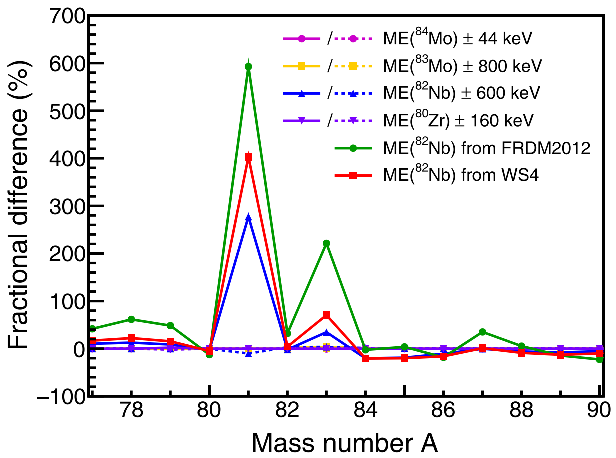

Fig. 2. (color online) Using the calculation results with AME2020 masses as a reference,the fractional difference of abundance as a function of mass number A. The solid and dashed lines represent the results obtained with the nuclide mass increased and decreased by 2σ deviated from the AME2020 central mass value, respectively. In addition, the results using the ^{82}Nb mass value from FRDM2012 [11] and WS4 [12] theoretical predictions are also presented.

Here, the first striking finding is that the quite large mass variations of ± 800 keV in ^{83}Mo still have a negligible impact on the final abundances. As illustrated in Fig. 3, although the large mass variations in ^{83}Mo alter the primary net flows beyond ^{82}Nb, these flows ultimately converge at ^{83}Nb with no significant leakage. This behavior is ensured by the short half-life of ^{83}Mo (23 ± 19 ms) and the long half-life of ^{82}Zr (32 ± 5 s), which channel the flow through ^{82}Nb(p, γ)^{83}Mo(β^+)^{83}Nb and ^{82}Nb(β^+)^{82}Zr(p, γ)^{83}Nb, respectively.

Another notable feature in Fig. 2 is that, for ^{82}Nb, a 2σ mass decrease has only a relatively minor influence on the calculated abundances, whereas a mass increase of the same magnitude leads to a pronounced change, particularly at $A = 81$. This asymmetry arises because, when the lower mass value of ^{82}Nb is used, as in the case with the central value, the forward ^{81}Zr(p, γ)^{82}Nb reaction dominates over its reverse for most of the time (see the red and

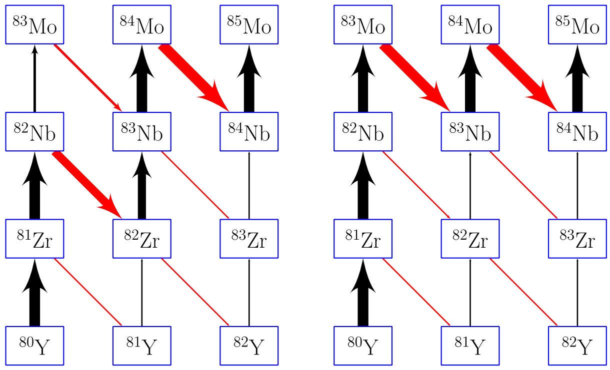

Fig. 3. (color online) The rp-process reaction net flow near ^{83}Mo. The thickness of these arrows indicates the strength of reaction flows. Left: ME(^{83}Mo) + 800 keV, Right: ME(^{83}Mo) - 800 keV.

green lines in Fig. 4). In contrast, when the higher mass value is adopted, the (p, γ)-(γ, p) equilibrium between ^{81}Zr and ^{82}Nb is more readily established (see the blue line in Fig. 4). This leads to a pronounced accumulation of ^{81}Zr, which in turn enhances the abundance at $A = 81$. Similarly, in Fig. 2, we also include a comparison using the predicted mass values of ^{82}Nb from FRDM2012 [11] (ME(^{82}Nb) = –50830 keV) and WS4 [12] (ME(^{82}Nb) = –51090 keV), together with that from AME2020 (ME(^{82}Nb) = –51810 keV). The higher mass value of ^{82}Nb corresponds to a larger fractional abundance difference at $A = 81$, which is consistent with the above analysis.

For ^{84}Mo and ^{80}Zr, although the mass uncertainties exceed 10 keV, the resulting ± 2σ variations in their S_p values remain small relative to the large S_p values themselves (see Table 1). This appears to be the primary reason why the mass uncertainties have only a minor effect on the fractional differences in the abundances.

III. THE EFFECT OF Zr-Nb CYCLE IN RP-PROCESS

When the flow returning to ^{80}Zr is comparable to the flow escaping the $N = 42$ isotonic chain owing to a sufficiently low mass value of ^{80}Zr, the Zr-Nb cycle emerges as an endpoint of the rp-process.

In Refs. [20, 24], to quantitatively estimate the contribution of the Zr-Nb cycle to the rp-process, a cycle branching ratio was defined as the fraction of the flow ending at ^{80}Zr via the ^{83}Nb(p, α)^{80}Zr and ^{84}Mo(γ, α)^{80}Zr reactions. In the more recent work of Ref. [20], the mass values of ^{80}Zr and ^{84}Mo were extrapolated. Then, a favorable condition was defined by assuming the 1σ upper or lower limits of the mass uncertainties that give the largest Q-value for the ^{83}Nb(p, α)^{80}Zr reaction and the minimum S_α(^{84}Mo). Under this favorable condition, the calculated branching ratio was several orders of magnitude lower

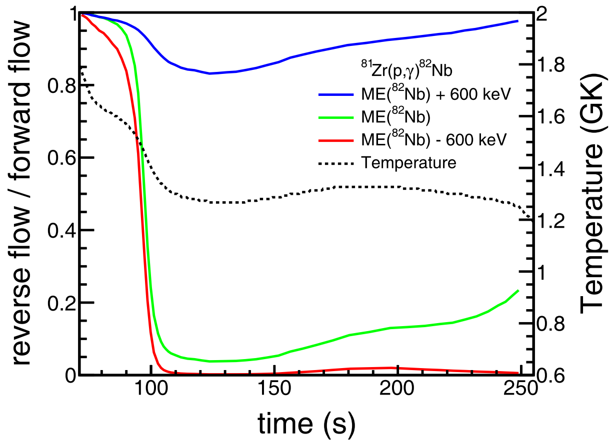

Fig. 4. (color online) Ratio of reverse to forward flow for ^{81}Zr(p, γ)^{82}Nb under different ^{82}Nb mass values, as a function of time. The temperature profile is also shown as the dotted line.

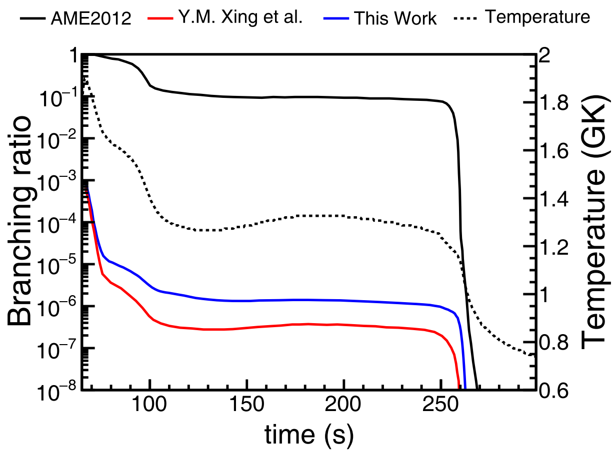

Fig. 5. (color online) Ratio of the reaction flows branching into the Zr–Nb cycle. The black and red lines are adopted from Ref. [20] (see text for details). The blue line is under the favorable condition with the masses of ^{80}Zr and ^{84}Mo being 2σ lower and upper over their central values, respectively.

than that obtained using the AME2012 mass values [28, 29] (see the red and black solid lines in Fig. 5 or Fig. 4 in Ref. [20]). As a result, the Zr-Nb cycle was believed either not to exist or, at least, to be much weaker than previously expected. However, the masses of ^{80}Zr and ^{84}Mo were later experimentally measured [22, 23] (see Table 1), and the S_α(^{84}Mo) was obtained as 1.434(83) MeV, almost 0.8 MeV lower than the extrapolated value in Ref. [20].

To demonstrate the effect of the new mass measurements of ^{80}Zr and ^{84}Mo on the Zr-Nb cycle, a more favorable scenario is assumed, in which the masses of ^{80}Zr and ^{84}Mo are respectively 2σ below and above their central values.

Under this more favorable condition, the branching ratio is shown by the blue line in Fig 5, confirming that the Zr-Nb cycle can be unambiguously excluded, even at the peak temperature of ~1.9 GK.

IV. SUMMARY

We have investigated the impact of current mass uncertainties of ^{83,84}Mo, ^{82}Nb, and ^{80}Zr on the final ash composition of the rp-process in XRBs. Our results reveal that the long half-life of ^{82}Zr plays an important role, rendering the large mass uncertainty of ^{83}Mo irrelevant to the abundances at $A = 82$ and beyond. In contrast, the mass uncertainty of ^{82}Nb exerts a significant influence on the $A = 81$ abundance, which is notably enhanced as the mass of ^{82}Nb increases. This finding highlights the particular importance of future high-precision mass measurements of ^{82}Nb for more accurate modeling of the rp-process. Furthermore, our results confirm that the Zr-Nb cycle remains negligible under the newly measured masses and associated uncertainties of ^{84}Mo and ^{80}Zr.

References

[1] Z. Meisel, G. Merz, S. Medvid, Astrophys. J. **872**, 84 (2019)
[2] H. Schatz, K. Rehm, Nucl. Phys. A **777**, 601 (2006)
[3] R. K. Wallace, S. E. Woosley, Astrophys. J. Suppl. Ser. **45**, 389 (1981)
[4] H. Schatz, A. Aprahamian, J. Gorres *et al.*, Phys. Rep. **294**, 167 (1998)
[5] C. Bertulani, T. Kajino, Prog. Part. Nucl. Phys. **89**, 56 (2016)
[6] L. P. Zhang, J. J. He, W. D. Chai *et al.*, Chin. Phys. C **40**, 125101 (2016)
[7] J. J. Liu, D. M. Liu, Chin. Phys. C **41**, 125102 (2017)
[8] H. Schatz, Int. J. Mass Spectrom. **251**, 293 (2006)
[9] H. Schatz, W.-J. Ong, Astrophys. J. **844**, 139 (2017)
[10] A. Parikh, J. José, C. Iliadis *et al.*, Phys. Rev. C **79**, 045802 (2009)
[11] P. Möller, W. D. Myers, H. Sagawa *et al.*, Phys. Rev. Lett. **108**, 052501 (2012)
[12] N. Wang, M. Liu, X. Wu *et al.*, Phys. Lett. B **734**, 215 (2014)
[13] P. Guo, X. J. Cao, K. M. Chen *et al.*, At. Data Nucl. Data Tables **158**, 101661 (2024)
[14] M. Wang, W. J. Huang, F. G. Kondev *et al.*, Chin. Phys. C **45**, 030003 (2021)
[15] A. Sobiczewski, Yu.A. Litvinov, M. Palczewski, At. Data Nucl. Data Tables **119**, 1 (2018)
[16] X. Zhou, M. Wang, Y. H. Zhang *et al.*, Nat. Phys. **19**, 1091 (2023)
[17] Z. Y. Chen, X. L. Yan, S. Q. Hou *et al.*, Astrophys. J. **994**, 270 (2025)
[18] G. Audi, F. G. Kondev, M. Wang *et al.*, Chin. Phys. C **41**, 030001 (2017)
[19] M. Wang, G. Audi, F. G. Kondev *et al.*, Chin. Phys. C **41**, 030003 (2017)
[20] Y. M. Xing, K. A. Li, Y. H. Zhang *et al.*, Phys. Lett. B **781**, 358 (2018)
[21] M. Vilén, A. Kankainen, P. Bączyk *et al.*, Phys. Rev. C **100**, 054333 (2019)
[22] A. Hamaker, E. Leistenschneider, R. Jain *et al.*, Nat. Phys. **17**, 1408 (2021)
[23] S. Kimura, M. Wada, C. Y. Fu *et al.*, Phys. Rev. Lett. **135**, 152701 (2025)
[24] E. Haettner, D. Ackermann, G. Audi *et al.*, Phys. Rev. Lett. **106**, 122501 (2011)
[25] M. J. Bojazi, B. S. Meyer, Phys. Rev. C **89**, 025807 (2014)
[26] H. Schatz, A. Aprahamian, V. Barnard *et al.*, Phys. Rev. Lett. **86**, 3471 (2001)
[27] S. Goriely, S. Hilaire, A. J. Koning, Astron. Astrophys. **487**, 767 (2008)
[28] G. Audi, M. Wang, A. H. Wapstra *et al.*, Chin. Phys. C **36**, 1603 (2012)
[29] G. Audi, F. G. Kondev, M. Wang *et al.*, Chin. Phys. C **36**, 1157 (2012)